First Principle Investigations of Long-range Magnetic Exchange Interactions via Polyacene Couplers

Prabhleen Kaur and Md. Ehesan Ali*

Institute of Nano Science and Technology, Phase 10, Sector-64, Mohali Punjab-160062, India

E-mail: ehesan.ali@inst.ac.in

Abstract

The electronic and magnetic properties of polyacenes become quite fascinating as the number of linearly conjugated benzene rings increases. Higher-order conjugated polyacenes develop radicaloid characters due to the transition of electronic structures from closed-shell to the open-shell system. Here we have investigated the role of such polyacenes as the magnetic coupler when placed between the two spin-sources based on nitroxy radicals. To do so, the magnetic exchange interactions ($2J$) are computed employing electronic structure theories, i.e. broken-symmetry (BS) approach within the density functional theory (DFT) as well as symmetry-adopted wave function based multi-configurational methods. In the former approach, various genre of exchange-correlation (XC) functionals such as generalized gradient approximation (GGA), meta-GGA, hybrid functional, constrained spin density (i.e. CDFT) and on-site Coulomb correlation corrected GGA+U functionals are adopted. All DFT based calculations estimate an exponential increase in $2J$ values with the length of the couplers, especially for the higher-order acenes. This is indeed an unexpected observation and also there is no experimental report is available in support of the DFT calculations. The complexity in the electronic structure enhances with the increasing number of benzene rings due to an increase

in near-degenerate or quasi-degenerate molecular orbitals (MOs) and also the reduction of the energy gap with the low-lying excited states. Consequently, it invokes a sever challenge in the computations of the magnetic exchange interactions in DFT. As an alternative approach, the wave function based multi-reference calculations, e.g. CASSCF/NEVPT2 methods are also adopted. In the later calculations, it has been realized that the π-orbitals of the couplers play a crucial role in the exchange interactions. For larger polyacenes (i.e. hexacene to decacene) such calculations become prohibitively expensive and rigorous as the number of π-orbitals increases, thus expanding the active space enormously. The limited active spaces calculations indicate quite strong exchange interactions, thus *in principle,* it supports the DFT observations of long-range magnetic exchange interactions, but not the exponential increase of $2J$ with the length of the couplers. In the current scenario, it is anticipated that a methodology that could account for the entire π-electrons in the active space such as CASSCF-DMRG like approach could resolve the issue.

Introduction

Molecular magnets based on the stable organic radicals have attracted enormous attention due to their potential applications in spintronics,[1] magnetic logic devices,[2] and quantum computers.[3] The non-magnetic spacer between the radical centers control the nature and strength of intramolecular magnetic exchange interactions.[4–6] The seamless π-conjugations between the radical centers and spacer play a vital role in magnetic couplings.[7–9] Strong magnetic exchange interactions are reported mostly for couplers with smaller lengths.[10] However, the fascinating long-range couplers desired[11,12] for magnetic and spintronic applications are relatively less explored. On the top of it accomplishment of long range strong magnetic exchange interactions in molecular system is another challenge. The exchange interactions through the larger molecular spacers were investigated by Matsuda et al. for various π-conjugated couplers and established a correspondence between electrical conductance and the magnetic exchange interaction.[13] Both the molecular conductance and the exchange interactions decay exponentially with an increase in distance between radical

centers. They observed that the increased π-conjugations slow down the decay process.[14,15] The strength of the magnetic exchange coupling constants ($2J$), mediated through π-conjugated molecular spacers was found to decay exponentially with the length of the couplers.[13]

The m-phenylene coupler unit is the most commonly used monomer fragment to device into stable ferromagnetic molecular units. Different nitronyl-nitroxide and nitroxide diradicals have been synthesized with the m-phenylene spacer. The influence of different structural parameters on magnetic exchange coupling has also been studied. A small distortion of planarity in the radical units and m-phenylene coupler changes magnetic coupling constant significantly. In a work by Rajca and co-workers, the lower limits for exchange couplings were found to be $>139\ cm^{-1}$ through EPR measurements in the solution phase. While, the same diradical systems exhibited different coupling values of $> 208\ cm^{-1}$ and 278-556 cm^{-1} in solid-phase depending on structural conformations.[16,17]

In the present work, we intended to investigate the long-range magnetic exchange interactions between the two localized radicals centers coupled through linear polyacene spacers. Polyacenes are highly conjugated systems with fused benzene rings and possess a rich and intricate electronic structure. Bendikov et al. discovered that in larger acenes the closed-shell nature of the non-magnetic acenes switches to open-shell electronic ground state.[18] They also predicted a transition in electronic structure from discrete molecular orbitals to band picture occurs for octacene onwards.[18] Such interconversion in the electronic structure in polyacenes has consequences on its ground state molecular properties such as optical[19], magnetic[20], vibrational,[21] and other spectroscopic properties[22]. Here such linear polyacenes are adopted as the spacers in coupling the conformationally restricted nitroxy-diradicals. The conformationally restricted di-radicals are specifically opted here to minimize the influence of torsional angles on magnetic coupling constant values. [23–26] The nitroxy radicals are connected at m-positions of the polyacene to have a ferromagnetic coupling between these radical centers. The spacer length is uniformly increased by adding a unit of fused benzene ring with **1** corresponding to diradical system with benzene coupler and **10** corresponding to diradical system with decacene coupler.

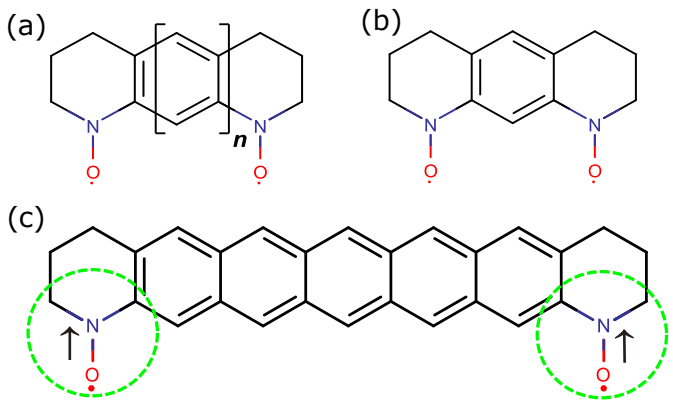

Figure 1: (a) Conformationally constrained nitroxy diradicals coupled through polyacene spacers varying ***n*** from 1 to 10. The corresponding diradicals are aliased as **1** to **10**. (b) Diradical **1** with polyacene spacer benzene bridged between the nitroxy diradicals. (c) Spin moment constraining zones (in green) constraining a moment of 1.00 μ_B used in CBS-DFT study represented here for triplet state of diradical **5**.

Theoretical and Computational Methodology

The complete series of diradicals *i.e.* **1-10** were optimized in triplet state within the density functional theory (DFT) framework adopting Becke's three-parameter and Lee-Yang-Parr's exchange-correlation hybrid functional (B3LYP).[27] The atom centred polarized triple-zeta (def2-TZVP) [28,29] basis set was used for all the atoms as employed in quantum chemistry code ORCA [30] with the convergence criteria of 10^{-8} Eh for each electronic steps. To speed up the calculations, resolution of the identity (RI) approximation along with the auxiliary basis set def2/J has been used with chain of spheres (COSX) numerical integration.[31] Since triplet was the ground state for all the diradicals, these B3LYP optimized geometries were used to compute the exchange coupling constants by performing single point calculations with different functionals.

The magnetic exchange interaction between the two magnetic sites A and B could be expressed by the Heisenberg-Dirac-Van Vleck (HDVV) spin Hamiltonian:

$$\hat{H}_{HDVV} = -2J\hat{S}_A.\hat{S}_B \tag{1}$$

where $2J$ is the orbital-averaged effective exchange integral between the spin sites A and B, $\hat{S}_A$ and

$\hat{S}_B$ being the respective spin operators of these sites. The positive sign of $2J$ indicates ferromagnetic and the negative sign indicates antiferromagnetic interactions. In diradicals, the exchange interactions could be extracted from the energy of the pure spin-states as

$$E_{S=0} - E_{S=1} = 2J \tag{2}$$

where $E_{S=1}$ and $E_{S=0}$ correspond to the energies of the triplet and singlet states respectively. In principle, the magnetic exchange interactions could be obtained applying Eq.2 for wave function based multi-reference *ab initio* calculations of spin multiplet energetics. However, in the spin-unrestricted Kohn-Sham $\big(\mathrm{UKS}\big)$ approach, it is not possible to obtain the pure singlet state because of the broken natural spin symmetry for open-shell singlets. This results in a poor description of the spin states energies as well as spin-contaminated states.[32–34] Ginsberg and Noodleman proposed a strategy to extract the exchange-interactions by mapping the eigen states of the Heisenberg spin Hamiltonian with the high spin-states and broken-symmetry states as obtained from the UKS solutions.[35] This is popularly known as the broken-symmetry (BS) method or more precisely standard broken-symmetry DFT method. The BS solution is not an eigenfunction of the Hamiltonian, but is an admixture of the singlet and triplet states. In principle, the singlet-state requires multi-determinant representation of the wave function which cannot not be obtained accurately in a single-determinant approach. However, standard broken-symmetry DFT is found to be a successful method in extracting the exchange interactions ($2J$) for the organic diradicals.[36,37] The following expression,

$$2J = 2\Big(\frac{E_{BS} - E_{HS}}{S^2_{max}}\Big) \tag{3}$$

is generally used to extract the $2J$ values in the broken-symmetry calculations and popularly known as Ginsberg-Noodleman-Davidson[35] approach. It produces accurate exchange interactions for the systems in which the Heisenberg exchange including the ligand-to-metal spin polarization and direct exchange interactions contribute predominantly in the magnetic exchange interactions. The overlap integral between the magnetic orbitals was neglected in this formulation. In the current

work, within DFT regime Eq. 3 were used for the evaluation of the exchange interactions whereas Eq. 2 was used to evaluate $2J$ from multi-reference based methods.

Density functional theory based calculations

The standard broken-symmetry DFT calculations were carried out adopting the proposition of Ginsberg and Noodleman et al.[38–40] that was also advocated by several groups.[41–43] The quantum chemistry code ORCA was used for all the standard broken-symmetry DFT calculations.[30]The computed $2J$ values for the different magnetic molecules strongly depend on the applied exchange-correlation functional within the DFT framework. Thus to obtain an in-depth understanding of the exchange interactions obtained from DFT calculations, a number of functionals from Jacob's ladder are selected. These include GGA (BLYP and PBE), meta-GGA (TPSS and M06-L) and hybrid (B3LYP (20% HF exchange), PBE0 (25% HF exchange) and M06 (27% HF exchange)) functionals. In addition to the aforementioned functionals, two other popular functionals (CDFT and GGA+U) but relatively less used by the community for organic diradicals are applied and described in the following sections.

Spin-Constrained density functional theory (CDFT)

In high-symmetric and planner magnetic molecules, the singly-occupied molecular orbitals (SOMOs) obtained in the DFT calculations are generally over delocalized due to self-interactions error (SIE) in DFT. Hence the spin moments aslo get delocalized from their localized radical centers. Such unphysical delocalization leads to the spurious description of the chemical bondings as well as associated molecular properties, especially for open-shell magnetic molecules. Recently, it has been observed that the spin-constrained DFT (CDFT) could rectify this to a certain extent.[44] In CDFT, the $\uparrow\downarrow$ state is obtained directly by minimizing the KS energy E^{KS} subject to the constraint that the spin of A $\left[\text{i.e., the difference between the number of} \uparrow \left(N_A^{\alpha}\right) \text{and} \downarrow \left(N_A^{\beta}\right) \text{electrons on A}\right]$

should be S_A, while the spin of B should be S_B:

$$N_A^\alpha - N_A^\beta = S_A, \qquad N_B^\alpha - N_B^\beta = S_B \tag{4}$$

For the $\uparrow\downarrow$ state, S_A is positive while S_B is negative and then Löwdin population is used to define $N_{A,B}^\sigma$. To perform the constrained minimization, two Lagrange multipliers were introduced $\left(\gamma_A, \gamma_B\right)$ and a new functional of electron density $\left(\rho\right)$ is optimized:

$$W\left[\rho_\alpha, \rho_\beta, \gamma_A, \gamma_B\right] = E^{KS}\left[\rho_\alpha, \rho_\beta\right] + \gamma_A\left(N_A^\alpha - N_A^\beta - S_A\right) + \gamma_B\left(N_B^\alpha - N_B^\beta - S_B\right) \tag{5}$$

where density is a sum of orbital densities,

$$\rho_\sigma\left(\mathbf{r}\right) \equiv \sum_i \left|\phi_{i,\sigma}\left(\mathbf{r}\right)\right|^2 \tag{6}$$

In the CDFT approach, this new functional W was optimized with respect to the Lagrange multipliers in addition to the spin-densities. CDFT single-point calculations were performed by localizing the spin-densities within the nitroxyl radical using B3LYP/6-31G(d) method as implemented in NWChem quantum chemistry code.[45,46] One has to be careful while performing the CDFT calculations, as the outcome depends strongly on the constrained spin-moments. Thus, to succeed in CDFT calculations, one has to identify the exact amount of localized spin-moments within certain spatial regions in the molecule. This is indeed a cumbersome task, but a systematic procedure was reported in our previous work.[47,48] In this work we have constrained $1.0\mu_B$ spin moments within the **-NO**$^\cdot$ regions for all the diradicals (**1** to **10**).

Hubbard-U corrected GGA+U functional

The GGA+U approach has been introduced as a method to treat excessive delocalization of d and f electrons of transition metal and rare earth element as predicted by standard GGA exchange-correlation potentials. The "U" treats the strong on-site Coulomb interaction of localized electrons

with an additional Hubbard-like term. The GGA+U functional may be formulated as follows:

$$E_{GGA+U}[\rho(\mathbf{r})] = E_{GGA}[\rho(\mathbf{r})] + E_U[n^{I\sigma}_{mm'}] \tag{7}$$

where $\rho(\mathbf{r})$ is the electronic density, $E_{GGA}[\rho(\mathbf{r})]$ is the standard GGA energy functional, $n^{I\sigma}_{mm'}$ are generalized atomic occupations (i.e. density matrix elements) with spin σ associated to the I atom, and $n^{I\sigma}$ is the sum of the occupations corresponding to all m and m' orbitals and $E_U[n^{I\sigma}_{mm'}]$ represents the correct and accurate value for the on-site correlation energy between electrons in the m and m' orbitals which belong to a given atomic shell (s, p, d, f, ...) centered at the same I atom. However, $E_{GGA}[\rho(\mathbf{r})]$ already contains an approximate estimate of electron correlation effects, including the on-site correlation energy between electrons in these m and m' orbitals, hence a term accounting for the GGA estimate of this electron-electron interaction, $E_{DC}[n^{I\sigma}]$, must be subtracted to avoid double counting when using a Hubbard scheme to represent this correction as in the following equation:

$$E_{GGA+U}[\rho(\mathbf{r})] = E_{GGA}[\rho(\mathbf{r})] + E_{HUB}[n^{I\sigma}_{mm'}] - E_{DC}[n^{I\sigma}] \tag{8}$$

Here, the $U_{eff} = U - J$ has been used to impose Hubbard's parameter on the radicals as proposed by Dudrarev et al.[49] where U is the on-site Coulomb term while J is the site exchange term (not the same as magnetic exchange coupling constant). Most often, the U_{eff} parameter in these approaches has been considered as an empirical parameter introduced to correct the deficiencies of the GGA exchange-correlation potentials in describing the charge (and spin) distributions of atoms involving d or f electrons. This on-site Coulomb correction can be applied to $2p$ electrons as well.

Herein, to take into account the delocalization of spin from radical centers PBE+U[50–52] was used to calculate the exchange coupling constant by adding on-site Hubbard's U parameter on the -NO$^{\cdot}$ radical centers. The pseudopotentials with projector augmented-wave (PAW)[53] methods were used with a kinetic energy cutoff of 400 eV. The Hubbard-U parameter was empirically varied in the range of 2 to 5 eV for all the diradicals. The exchange interactions was obtained applying the

broken-symmetry methods.[54,55] The GGA+U calculations were performed in VASP[56] by placing the diradical in a periodic large rectangular cuboid box (for e.g. 17.00 x 17.00 x 12.00 $\AA^3$ for **1** to 27.00 x 27.00 x 15.00 $\AA^3$ for **10**) to avoid spurious interaction between the periodic images. The cell size chosen for all the diradicals was such that the images were at least 10Å apart in all the directions. The exam same amount of on-site Hubbard-U was applied to the $2p$-orbitals of both N and O-atoms, that primarily host the unpair electron and behave as spin-centers. The $2J$ values discussed in the main text are with U_{eff} =2 eV, the rest are provided in SI (Table S13).

Multi-configurational calculations

The multi-configurational calculations are essential for computing the magnetic exchange interactions ($2J$) in the wave-function based methods mainly to account the electron-correlation energies, especially for the highly-correlated magnetic systems. The presence of low-lying excited states, quasi-degenerate or degenerate molecular orbitals (MOs) and the multi-determinant nature of the open-shell singlet (anti-ferromagnetic) states are the other reasons to consider the multi-configurational methods. Thus, in addition to the DFT calculations, we also computed the magnetic exchange interactions employing the complete active space self-consistent field (CASSCF) method that accounts the static electronic correlations for the chosen active space.[57–59] The static correlations are mainly long-range in nature while the dynamical correlations are short-ranged type. The effect of dynamical electronic correlations on the magnetic exchange interactions is accounted through the n-electron valence state perturbation theory (NEVPT2).[60,61] The NEVPT2 methods incorporate the dynamical correlations through the second-order perturbative treatment of the CASSCF optimized wave-functions in the selected CAS spaces. All the CASSCF and CASSCF/NEVPT2 calculations with different active spaces were performed in ORCA software package.[30]

Results and Discussions

The computed exchange interactions for all **1**–**10** diradicals employing different functionals are tabulated in Table 1. The conformationally restricted nitroxy diradical with *m*-phenylene coupler similar to diradical **1**, was reported by Rajca and co-workers. Employing ESR spectroscopy, the authors could observe the lower limit of the magnetic coupling constants of $>202\ cm^{-1}$.[16] However, the $2J$'s obtained with different DFT functionals for **1** are substantially varied between 174 –1356 cm^{-1} for different functionals. The lowest value for coupling constant is observed with CBS-DFT, but all other functionals produce $2J$ between 580 to 1356 cm^{-1} for diradical **1**. Whereas CBS-DFT(B3LYP) produces 174 cm^{-1}, which is much closer (but slightly underestimated) to the experimentally observed value of (>202 cm^{-1}) by Rajca et al. compared to BS-DFT(B3LYP) that produces 1127.94 cm^{-1}. This indicates that CDFT produces much better coupling constant compared to the standard DFT calculations. A modelled nitroxy-diradical coupled through the substituted *m*-phenylene coupler similar to diradical **1** was previously investigated by Ali et al. applying standard broken-symmetry DFT and CAS-CI methods.[62] It was observed that the standard BS-DFT consistently overestimate the exchange interactions, and this is a general trend in DFT based calculations, specially for the radicals in which the spin-centers are coplanar with the conjugated molecular spacers.[63–65] The computed $2J$ values using the DFT functionals as tabulated in Table 1 for all the diradicals **1**–**10** follow a general trend such as $2J$(CBS/CDFT) $< 2J$(GGA)$< 2J$(GGA+U) $< 2J$(meta-GGA) $< 2J$(hybrid-GGA).

The other interesting observation in Table 1 is the $<S^2>$, that increases (for both the spin-states) with the increase in number of benzene rings. The deviations of $<S^2>$ from its expected values indicate the spin-contamination that generally occurs due to the mixing of low-lying states. To extract the $2J$ values from the strongly mixed states, Yamaguchi's proposition of spin-projection method is also applied[41]. (Table S2, SI)

The comparisons of $<S^2>$ values between the BS-DFT and CBS-DFT indicates the resulting spin-sates are closer to pure spin-state for CDFT (till **5**) compared to hybrid functionals in the standard DFT formalism. In this context, we would like to draw the attention of the readers to

surprisingly better performance for the GGA and meta-GGA functionals compared to the hybrid-functionals which is also reflected in their $<S^2>$ values as well. The better performance for GGA and meta-GGA functionals in terms of $2J$ and $<S^2>$ values are incidental due to less mixing with the excited states and also due to more $spin-spilling$ that will be discussed in the later sections.

Magnetic exchange interactions vs length of the couplers

In previous reports Ali et al.[66] and Bhattacharya et al.[67] investigated the role of linear acene couplers in magnetic exchange interaction, that indicated the increase in coupling constant with increase in the lengths of the couplers, though the investigations in both of these studies were limited up to the pentacene couplers only. In this study, the density based methods (irrespective of their genre of exchange-correlations functionals) we observed that the magnetic exchange interactions increases exponentially for the higher-order of polyacene couplers. (See Table 1 and Fig. 2) This observation is indeed very unusual and also goes against the general understanding of exchange interactions that usually decay either slowly or strongly depending on the nature of the couplers. A similar observation of increase of $2J$ values with the length of cumulene couplers was reported by Sarbadhikary et al. using broken-symmetry DFT calculations.[68] However, to best of our knowledge, till date there is no experimental confirmation/indication is available in favor of such theoretical observations. On the other hand Nishizawa and co-workers have reported the exponential decay of the magnetic interaction along the length of the couplers.[14] Thus, the DFT observations of exponential increase in $2J$ values with the lengths of the couplers seems to be paradoxical, that needs an in depth investigations unravelling the electronic structures of the higher-order polyacene couplers.

The spin density of broken symmetry states as obtained from standard BS-DFT (B3LYP) formalism is compared with those obtained from CBS-DFT(B3LYP). (see Table 2) Visually quite similar spin-densities are observed for diradicals **1** to **8** and deviations are noted from diradical **9** onwards. For diradical **10**, an abrupt failure of BS-DFT is observed in producing opposite spin-densities localized at both the -NO magnetic centers in the antiferromagnetic states. In this respect,

Table 1: Computed magnetic exchange coupling ($2J$) values and corresponding $<S^2>$ values of triplet (HS) and broken-symmetry (BS) states for all the diradicals (**1**-**10**) with various DFT based methods.

	$2J(cm^{-1})$ $<S^2>_{HS}$ ($<S^2>_{BS}$)					
Diradical	BLYP[a]	TPSS[a]	B3LYP[a]	M06[a]	CBS-DFT[b]	PBE+U[c]
1	580 *2.01* (*0.97*)	917 *2.02* (*0.98*)	1128 *2.03* (*1.00*)	1356 *2.04* (*1.00*)	174 *2.01* (*1.01*)	719
2	455 *2.01* (*0.98*)	699 *2.02* (*0.99*)	869 *2.05* (*1.01*)	1037 *2.06* (*1.01*)	173 *2.02* (*1.01*)	559
3	502 *2.02* (*0.99*)	766 *2.04* (*0.99*)	907 *2.08* (*1.02*)	1064 *2.09* (*1.02*)	208 *2.03* (*1.01*)	601
4	630 *2.03* (*1.00*)	893 *2.07* (*1.01*)	1115 *2.14* (*1.03*)	1298 *2.17* (*1.04*)	294 *2.06* (*1.02*)	709
5	831 *2.06* (*1.01*)	1173 *2.11* (*1.02*)	1536 *2.27* (*1.06*)	1764 *2.32* (*1.07*)	530 *2.16* (*1.02*)	956
6	1229 *2.10* (*1.00*)	1618 *2.20* (*1.04*)	2262 *2.47* (*1.10*)	2570 *2.52* (*1.12*)	1212 *2.43* (*1.04*)	1353
7	1554 *2.17* (*1.03*)	2248 *2.33* (*1.07*)	3288 *2.70* (*1.17*)	3653 *2.77* (*1.20*)	2484 *2.47* (*1.07*)	1891
8	2075 *2.26* (*1.05*)	2857 *2.47* (*1.27*)	4425 *2.93* (*1.31*)	4807 *3.01* (*1.37*)	4034 *2.99* (*1.15*)	2487
9	1653 *2.35* (*1.23*)	2609 *2.62* (*1.42*)	5446 *3.14* (*1.53*)	5822 *3.22* (*1.61*)	1563 *3.19* (*2.15*)	3288
10	1563 *2.45* (*1.29*)	2610 *2.76* (*1.50*)	5490 *3.32* (*1.95*)	6538 *3.42* (*2.01*)	6361 *3.37* (*1.78*)	– [d]

[a]basis set used for these calculations is def2-TZVP, [b]method used is B3LYP/6-31G*, [c]U_{eff} = 2 eV, [d]the calculations did not converge to proper spin state

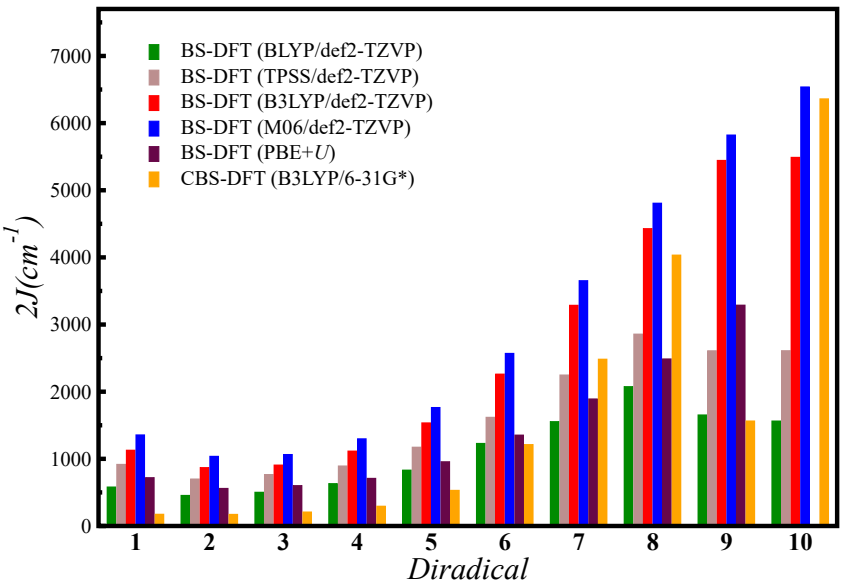

Figure 2: Comparison of the exchange interactions as computed in the density based methods. CDFT produced better 2*J* values compared to standard broken-symmetry DFT. However, both the methods produced unphysical high exchange interactions for the diradicals with larger polyacene couplers.

CDFT(CBS-DFT) turned out to be a successful and convenient method even for **10** especially to obtained a desired magnetic state. Moreover, spin density plots also reveal that for the larger acenes (**6/7** onwards) the central parts of the spacer slowly gained spin-polarization with the increased number of benzene rings. This is a direct consequence of the increasing open-shell nature of the couplers and development of radicaloid characters in the spacers. Therefore, a considerable amount of spin-density is found to be in the central region of the spacer in **10**. In the previous section, it was established that the GGA and meta-GGA seemed to perform better than hybrid functionals, however, these functionals in the BS-DFT approach even failed to achieve the desired BS state for diradical **9** also. (Table S10) Whereas CDFT overcomes such issues and the desired BS states are achieved for all the diradicals.

The $<S^2>$ values of the converged BS and high-spin (HS) states for diradicals **1** to **4** indicate the smooth convergence of the wave functions with expected values of $\sim$2.00 for triplet HS state and $\sim$1.00 for BS state. The deviation in $<S^2>$ generally occurs due to spin contaminations. As the ground spin-state of all the studied diradicals is triplet, we will restrict our discussion only for

Table 2: Spin density distributions of the broken symmetry state extracted from BS-DFT and CBS-DFT for diradicals **1**-**10**

	BS-DFT	CBS-DFT
1	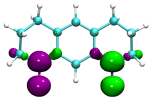	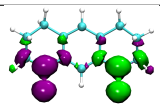
2	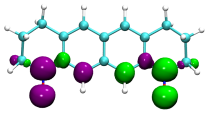	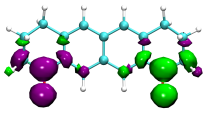
3	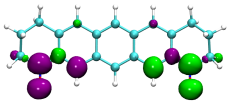	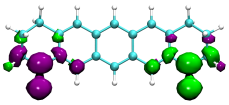
4	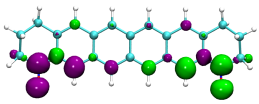	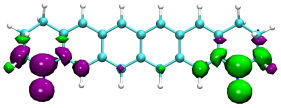
5	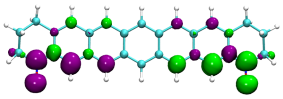	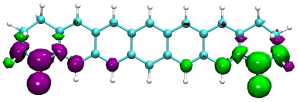
6	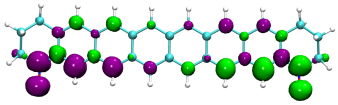	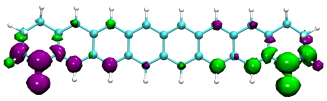
7	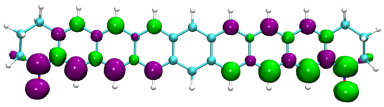	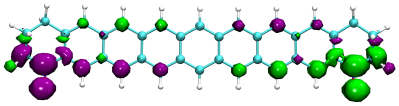
8	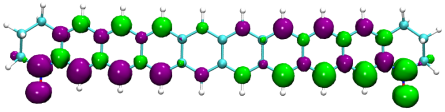	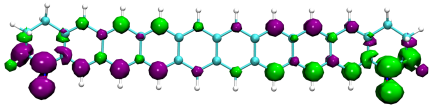
9	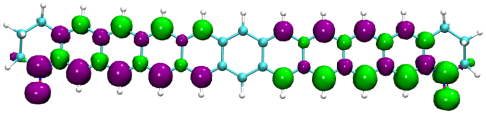	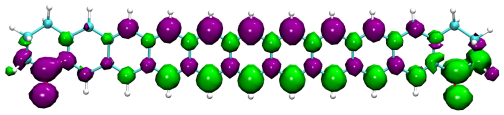
10	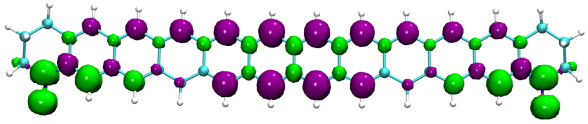	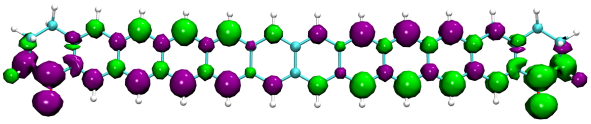

triplet state. As the benzene rings in the coupler increases, the molecular wave functions start to deviate from its pure spin state i.e. $S = 1$ for triplet state. This is reflected in the computed $<S^2>$ values as given in Table 1. One of the reasons for such high contamination is the enhanced de-

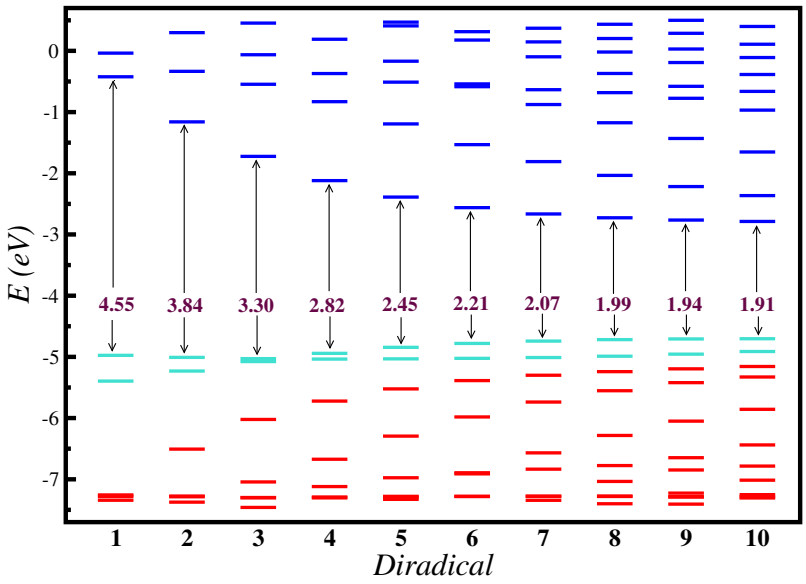

Figure 3: Molecular orbitals of spin-up electrons of all the diradicals in the energy range of -7.5 eV to 0.5 eV. The doubly occupied, singly occupied and unoccupied orbitals are represented by red, cyan and blue colors respectively.

generacy of the molecular orbitals as n increases. Figure 3 depicts the orbital energy levels in the energy window of -7.5 eV to 0.5 eV. This orbital energy diagram plot indicates that the singly occupied molecular orbitals (SOMOs), the orbitals containing the unpaired electrons responsible for the magnetic properties of the molecules are almost pinned at same energy for all the diradicals **1** to **10**. The major change is observed for doubly occupied and un-occupied orbitals wherein the density of MO's increases with n. The other impact with the increased densities of the orbitals is that with unoccupied energy levels rapidly gets stabilized and come in close proximity to the pinned SOMOs. Thus HOMO(SOMO)-LUMO energy gaps also decreases along the increase number of benzene rings from **1** to **10**. All these facts indicate the increased degeneracy of the MOs. This is an issue as the single-determinant methods e.g. HF or DFT face dificulties.[69] Employing CDFT, the $<S^2>$ values improved slightly, but a remarkable improvement of the exchange interactions could be observed for the smaller acene couplers **1**–**5** (see Table 1). We observed that CDFT also

starts to deviate as the conjugation of the couplers increases i.e. diradical **5** onwards. This deviation could be attributed to the fact of natural breakdown of the single-determinant based wave functions as the degeneracy of the molecular orbitals increases as mentioned earlier. Even though CDFT method did successfully converged to the broken symmetry state for **10**, the $2J$ value is still comparable to that obtained from standard broken-symmetry DFT.

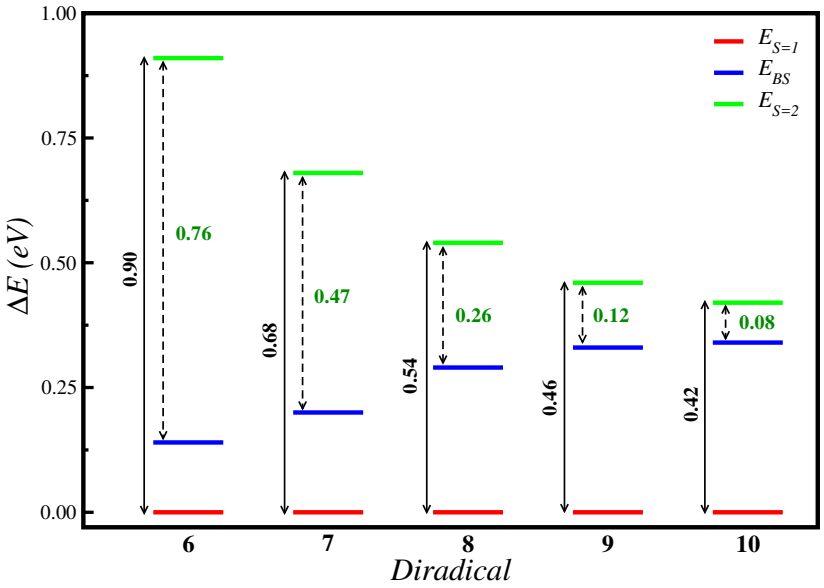

Figure 4: Relative energies of broken symmetry (BS) state (in blue) and quintet (S=2) state (in green) with respect to energy of triplet (S=1) ground state (in red) for diradicals **6**-**10**. With increase in coupler length, the energy gap between quintet-triplet and quintet-BS decreases. (Absolute energy values are given in SI)

The other reason for the spin-contamination is the mixing with the low-lying excited spin state especially for the longer polyacene couplers. For example, $<S^2>_{BS}$ for **10** approximately 2.00 is observed using hybrid functionals, which is almost equivalent to the expected $<S^2>$ value for a triplet state. For a diradical system the genesis of broken-symmetry occurs due to mixing of pure singlet and triplet multiplets. However, the $<S^2>$ values of **10** for the BS/HS states are $\sim$1.95/3.32 indicating that the resulting ground spin state is also not a pure spin state due to mixing with the low lying excited states. The success of the broken-symmetry methods are evident when at least the high-spin state is free from any spin-contaminations i.e. pure-spin state. However,

here we observed that the higher-spin states are not pure spin-sate as it get mixed with the quintet (S=2) state. Furthermore, the large spin contamination in both, the triplet as well as the broken-symmetry state is also due to quintet state which can be understood from the plot of quintet state energies relative to triplet state (which is ground state for all the cases) as shown in Figure 4. All the considered functionals reveal qualitatively similar trend of lowering of quintet state energy with respect to the ground state of the molecular systems (Figures S1-S7 and S10-S11, SI). Upon increasing the coupler length, the corresponding energy gap between the quintet-triplet states and quintet-BS states decreases respectively. Therefore, with the increase in coupler length, quintet state also starts to play an important role by being energetically close to the ground and BS state and thus, mixing with them. Thus far, it can be concluded that the orbital degeneracy of individual molecule and mixing from higher excited state are crucial factors that can not be directly taken into account.

The acenes are well known to develop open-shell character upon increase in its length, with open-shell-singlet (OSS) as its ground state. This increasing radical character of the couplers to some extent could also contribute in the spin-contamination of BS and triplet states of the diradicals **1**-**10**. Cano *et al*. have shown the effect of increasing open shell character of acenes escalating the spin contamination in both the triplet and BS states with dinuclear copper(II) systems.[70] Applying *ab initio* calculations here we have quantified the radicaloid characters (y-value) of the pristine polyacene as well as for polyacene in diradicals **1**-**10** where it acts as a coupler between -NO radical sites and tabulated in Table 3. This has been calculated following the work of Yamagucghi et al.[71] and details of calculations could be found in SI. As illustrated in Table 3 for pristine polyacene, the radicaloid nature increases with the increase of the number of benzene rings from 0.004 for benzene to 0.92 for the decacene. However, on placing between the spin centers, *i.e*., polyacene as coupler, the radical character decreases in comparison to pristine polyacene such that it significantly reduces to $y_c = 0.73$ in **10** from $y_p = 0.92$ in pristine form of decacene. This decrease in the radicaloid characters of the polyacene in the diradicals clearly reveals the *spin spilling* from the spin-center to the polyacene couplers.

Table 3: Computed diradical character of the polyacene in the pristine form (y_p) and as a coupler (y_c) in the diradical systems **1**-**10**.

no. of Benzene rings	pristine polyacenes (y_p)	polyacenes as coupler (y_c)
1	0.004	0.012
2	0.04	0.04
3	0.13	0.12
4	0.26	0.22
5	0.39	0.33
6	0.53	0.44
7	0.69	0.54
8	0.79	0.66
9	0.86	0.68
10	0.92	0.73

The phenomena of *spin spilling* can be visually anticipated from spin density plots (Table 2) and also from the value of net μ_B on the radical centers (Figure 5). Comparing the magnetic moments on the radical sites, it is observed that the hybrid functionals perform better in localizing the spin moments. Analyzing the spin density plots in Tables 2, S10 and S14, spin density in coupler can be seen increasing with maximum spin moment on carbons near the $-NO^{\cdot}$ spin centers. For higher conjugated systems *i.e.* **9** and **10**, the delocalized spin density in the center of the coupler owns to the OSS nature of the coupler. CBS-DFT method surpasses the phenomena of *spin-spilling* as the magnetic moment value remains constant for all the diradicals. The ease in spin-spilling is facilitated for studied systems by the fact that the magnetic orbital (p_z) are in plane with the π orbitals of the spacer.

To summarize the section, the calculations of $2J$ adopting the density based methods and mapping of the Heisenberg spin Hamiltonian is quite challenging task due to the complicated electronic structures of the higher order polyacene spacers. Thus one has to be careful to conclude about the $2J$s in such cases as obtained from the DFT calculations. To circumvent, the observed issues in DFT, we also performed the wave function based multi-reference calculations for these systems but that faces different challenges, which has been described in the following section.

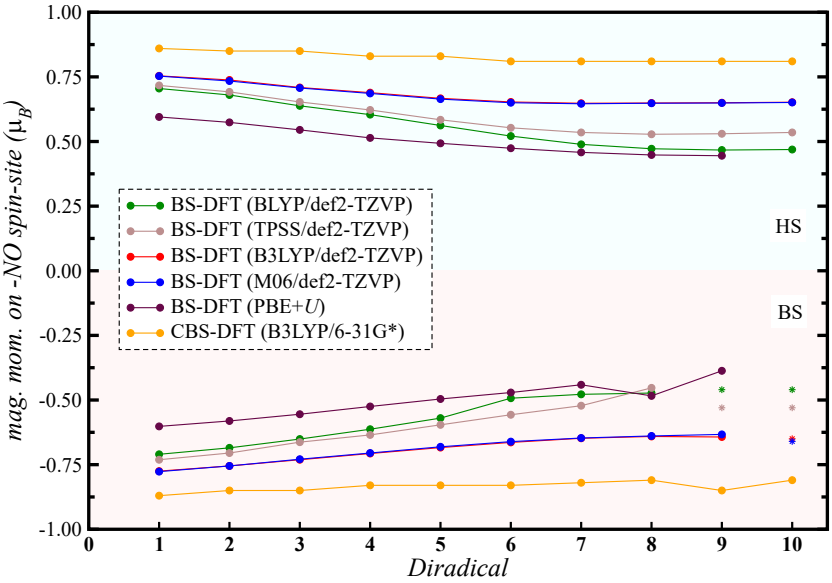

Figure 5: Magnetic moment on one of the radical sites (*i.e*. the site on which the magnetic moment reverses in BS state) with different functionals used. The positive and negative values correspond to the magnetic moment on *-NO* in HS (triplet) and BS state respectively. In few cases proper BS state was not achieved for diradicals **9** and **10** providing same sign for spin density on both the radical centers in the structure. The magnetic moments as obtained in BS state for those cases is marked with star by reversing the spin moment sign.

Multi-reference calculations

The multi-configurational CASSCF/NEVPT2 methods are quite successful in calculations of the 2*J* values. However, the choice of the active space is always a matter of concern for such calculations. In our previous work[65,72] and from several report in the literature, it has been realized that the minimal active space i.e. CAS(2,2) are quite successful in computing the magnetic exchange interactions in various organic diradicals when both SOMOs involves both the radical sites and coupler as well. In the minimal CAS approach, only the magnetic orbitals i.e. singly-occupied molecular orbitals (SOMOs) and the two unpaired electrons responsible for the magnetic centers are considered. The inclusion of static and dynamical correlations within the CAS(2,2) space remarkably produces the large part of the exchange interactions. Apart from the estimation of 2*J* values by CASSCF(2,2)/NEVPT2, we also realized that increasing the active space does not necessarily improves the 2*J* values remarkably. We trace down the issue as the imbalance accounting of the correlation energies between the ground state and the low lying excited state with the increases

of the active space. The imbalance occurs as the ground state becomes more stable compared to the excited states and as a results it produce large $2J$ values.

Table 4: Calculated exchange coupling constant, $2J$ (cm^{-1}) as obtained from CASSCF and CASSCF-NEVPT2 calculations for different diradicals with ROHF based active space orbitals.

	CAS(2,2)		CAS(4,4)		CAS(6,6)	
Diradical	CASSCF	NEVPT2	CASSCF	NEVPT2	CASSCF	NEVPT2
1	130.15	554.39	229.35	854.41	518.39	1353.06
2	48.54	246.68	79.88[a]	330.55	159.39	627.45
3	19.75	118.95	53.55	249.32	61.45	300.42
4	8.55	56.62	71.76	349.62	55.78	262.72
5	3.73	28.79	10.75	84.93	19.35	146.98
6	1.53	14.04	20.19	119.17	11.19[b]	53.39
7	0.65	6.80	2.63	-0.21	5.85	33.06
8	0.21	3.89	7.46	54.42	28.55[c]	195.96
9	0.11	0.42	0.65	-8.21	1.97	17.76
10	0.02	0.87	3.07	31.16	8.65[d]	64.12

[a,b,c,d] two set of orbitals satisfied the selection criterion. More details in SI.

The computed exchange interactions in the multi-configurational methods such as CASSCF and CASSCF-NEVPT2 with different active spaces for all the ten diradicals are given in Table 4. The minimal active space CAS(2,2) calculations were performed using the magnetic orbitals i.e. SOMOs localized on the -$NO^{\cdot}$ magnetic subunits. The computed exchange interactions employing CASSCF/NEVPT2 methods produces $2J$ values that decrease with the length of the couplers. This is in complete contrast to the prediction by DFT based calculations, where an exponential increase in $2J$'s with respect to the length of the couplers is observed. As mentioned earlier, the CASSCF(2,2)-NEVPT2 was observed to be an acceptable method to compute the magnetic exchange interactions for organic diradicals. However, a close look into the magnetic orbitals reveals that with the increase of the couplers lengths, the overlap of the magnetic orbitals reduces, thus the exchange interactions expectedly decreases, as CAS(2,2) space does not take into account the contribution from other π-orbitals.Thus the outcome of the CAS(2,2) calculations is artifact of the limited active space and could not be considered as physical observations, thus the extended active space are necessary for such polyacene couplers.

Therefore, further active space (4,4) and (6,6) are chosen by incorporating the orbitals contributing from the center of the acene couplers. For all the diradicals $2J$ values for the individual diradical increases with the increasing active space (except for **4** and **6** with (6,6) active space), this observation matches with the previous discussion and reports as well. The same holds true for CASSCF-NEVPT2 method as well. On increasing the size of active space to (4,4) and (6,6), the complete series show an even-odd effect. For (4,4) space, in odd-acene series it is the central benzene unit that contributes majorly. While, in even-acene series the central naphthalene unit of the individual systems play a vital role. Along the individual series with (4,4) active space we observe a continuous decrease in the exchange coupling constant values. Similar even-odd effect is observed even when the active space is (6,6), odd-acene series has major role of central anthracene unit in the individual spacers. Therefore, along odd-series with (6,6) space too we observe a continuous decrease in the magnetic exchange. The scenario is somewhat different with even-acene series in (6,6) space. Diradicals **2**, **4** and **6** have central naphthalene unit contribution to the active space while for **8** and **10** this contribution is from central tetracene unit. This revelation is important here, as in literature the boundary of the originating open-shell ground state for oligoacene is roughly established at heptacene [18,73,74] and the delocalized radical also has the similar qualitative appearance.[75,76] The exchange coupling constant values in this even-acene series decreases in going from **2** to **4** to **6** but increases in going from **6** to **8**. This sudden rise in the coupling constant could possibly the effect of the open shell diradical nature of the coupler that might come into play for such longer polyacene.

The study so far is incomplete to arrive at a conclusion for such highly correlated systems. Even in the limited CAS space it was difficult to go beyond (6,6) as the larger systems became not only more resource extensive but also the defining criteria to choose the active space was no longer simple. This still opens the door towards exciting physics that might be at play and may help in designing organic molecular systems with intrinsic radical character that might act as boosters to enhance the communication between the spin centers over long distances. Still, its a long way to go and other higher-level studies like DMRG along with experimental realization are required to

have better understanding for such systems.

Conclusions and outlook

The first principle calculations of magnetic exchange interaction for organic diradicals with higher-order linear polyacene couplers turned out to be the most challenging task due to the intriguing electronic structures of the spacers. The radicaloid characters, intrinsic open-shell electronic structure, presence of quasi-degenerate MOs, and the low-lying excited spin-sates add up to the complexity in the polyacene couplers. The order of complexity increases in many-folds with the increase of π-conjugations as the fused benzene rings increases. We further realized that the conformationally restricted planar radical moieties that are conjugated with couplers π-conjugations of the spacers facilitate *spin-spilling* into the spacers, which further invoke the additional challenges in the density-based calculations. However, CDFT prevents such spin-spilling and produces slightly smaller (or may be better) $2J$s in comparison to other BS-DFT methods. Eventually, CDFT for higher-order polyacene couplers also converged as of BS-DFT and produces an exponential increase in $2J$ values with the increase length of the couplers. The exchange interactions seems to be strongly influenced by radicaloide nature and the spin-spilling into the spacer. This indicates a much richer physics of exchange interaction mechanism that needs to be understood appropriately with further studies. Additional developments in theoretical methodologies to circumvent the observed issues in DFT are also foreseen.

The multi-configurational methods including dynamical electronic correlations are also severely limited especially for the higher-order acenes due to its requirements of prohibitively large and tedious active spaces. The minimal active space calculations reproduce opposite trends of $2J$ values to DFT calculations, however, it clarifies the importance of the CAS spaces steaming especially form the central part of the couplers. The extended active space indeed reproduces a much higher $2J$ values compare to CAS(2,2) calculations. However, the systematic inclusion of different MOs in the CAS space and their resulting $2J$ indicates a reasonably larger exchange interaction even with

the larger decacene coupler. To obtain more reliable or exact numerical values for $2J$, the complete *pi*-electrons should be accounted in the CAS space. Currently, we are aiming for CASSCF-DMRG calculations that is capable to handle quite a large active space as the extension of this work.

In a nutshell, despite the pragmatic difficulties in the computational methodologies, substantially strong-ferromagnetic exchange interactions (if not the exponential increase) for the higher-order acene couplers have been realized. The magnetic couplings through the OSS polyacene couplers are long-range in nature. Such systems will play a pivotal role in designing the ferromagnetic material with long-range magnetic orders. The participation of the spilled-spins (electrons) into the conduction band enhances such long-range exchange interactions between the spin-sites localized in the distance apart. Thus the synthesis of such organic diradicals with the polyacene couplers, will not only resolve the discussed dilemma, but it will open up a new avenue for the long-range magnetic materials.

Acknowledgement

We thank Peter M. Oppeneer for helpful discussion and Ashima Bajaj for her critical comments on the manuscript. Financial support from Department of Science and Technology through SERB-ECR project No. ECR/2016/000362, India-Sweden joint project No. DST/INT/SWD/VR/P-01/2016.

Supporting Information Available: Details of spin-constraint DFT, HOMO-LUMO energy gaps, spin-density plots for standard broken-symmetry DFT and CDFT, Selected active orbitals for multi-reference calculations This material is available free of charge via the Internet at http://pubs.acs.org.

References

(1) Wolf, S. A.; Awschalom, D. D.; Buhrman, R. A.; Daughton, J. M.; von Molnár, S.; Roukes, M. L.; Chtchelkanova, A. Y.; Treger, D. M. Spintronics: a spin-based electronics

vision for the future. *Science* **2001**, *294*, 1488–1495.

(2) Bogani, L.; Wernsdorfer, W. Molecular spintronics using single-molecule magnets. *Nat. Mater.* **2008**, *7*, 179–186.

(3) Rocha, A.; Garcia-Suarez, V.; Bailey, S.; Lambert, C. J.; Ferrer, J.; Sanvito, S. Towards molecular spintronics. *Nat. Mater.* **2005**, *4*, 335–339.

(4) Stroh, C.; Ziessel, R.; Raudaschl-Sieber, G.; Kohler, F. H.; Turek, P. Intramolecular exchange interactions in non-aromatic bis-nitronyl-nitroxides. *J. Mater. Chem.* **2005**, *15*, 850–858.

(5) Zeng, Y. F.; Hu, X.; Liu, F. C.; Bu, X. H. Azido-mediated systems showing different magnetic behaviors. *Chem. Soc. Rev.* **2009**, *38*, 469–480.

(6) Ziessel, R.; Stroh, C.; Heise, H.; Khler, F. H.; Turek, P.; Claiser, N.; Souhassou, M.; Lecomte, C. Strong exchange interactions between two radicals attached to nonaromatic spacers deduced from magnetic, EPR, NMR, and electron density measurements. *J. Am. Chem. Soc.* **2004**, *126*, 12604–12613.

(7) Rajca, A. Organic diradicals and polyradicals: from spin coupling to magnetism? *Chem. Rev.* **2002**, *94*, 871–893.

(8) Abe, M. Diradicals. *Chem. Rev.* **2013**, *113*, 7011–7088.

(9) Malrieu, J. P.; Caballol, R.; Calzado, C. J.; de Graaf, C.; Guihéry, N. Magnetic interactions in molecules and highly correlated materials: physical content, analytical derivation, and rigorous extraction of magnetic hamiltonians. *Chem. Rev.* **2014**, *114*, 429–492.

(10) Rajca, A.; Takahashi, M.; Pink, M.; Spagnol, G.; Rajca, S. Conformationally constrained, stable, triplet ground State (S = 1) nitroxide diradicals. Antiferromagnetic chains of S = 1 diradicals. *J. Am. Chem. Soc.* **2007**, *129*, 10159–10170.

(11) Pardo, E.; Faus, J.; Julve, M.; Lloret, F.; Muñoz, M. C.; Cano, J.; Ottenwaelder, X.; Journaux, Y.; Carrasco, R.; Blay, G.; Fernández, I.; Ruiz-García, R. Long-range magnetic coupling through extended π-conjugated aromatic bridges in dinuclear copper (II) metallacyclophanes. *J. Am. Chem. Soc.* **2003**, *125*, 10770–10771.

(12) Castellano, M.; Ruiz-García, R.; Cano, J.; Ferrando-Soria, J.; Pardo, E.; Fortea-Pérez, F. R.; Stiriba, S.-E.; Julve, M.; Lloret, F. Dicopper (II) metallacyclophanes as multifunctional magnetic devices: a joint experimental and computational study. *Acc. Chem. Res.* **2015**, *48*, 510–520.

(13) Higashiguchi, K.; Yumoto, K.; Matsuda, K. Evaluation of the β value of the phenylene unit by probing exchange interaction between two nitroxides. *Org. Lett.* **2010**, *12*, 5284–5286.

(14) Nishizawa, S.; Hasegawa, J.; Matsuda, K. Theoretical investigation of the β value of the π-conjugated molecular wires by evaluating exchange interaction between organic radicals. *J. Phys. Chem. C* **2013**, *117*, 26280–26286.

(15) Nishizawa, S.; Hasegawa, J.; Matsuda, K. Theoretical investigation of the β value of the phenylene and phenylene ethynylene units by evaluating exchange interaction between organic radicals. *Chem. Phys. Lett.* **2013**, *555*, 187–190.

(16) Rajca, A.; Shiraishi, K.; Rajca, S. Stable diarylnitroxide diradical with triplet ground state. *Chem. Commun.* **2009**, 4372–4374.

(17) Rajca, A.; Takahashi, M.; Pink, M.; Spagnol, G.; Rajca, S. Conformationally constrained, stable, triplet ground state (S = 1) nitroxide diradicals. Antiferromagnetic chains of S = 1 diradicals. *J. Am. Chem. Soc.* **2007**, *129*, 10159–10170.

(18) Bendikov, M.; Duong, H. M.; Starkey, K.; Houk, K. N.; Carter, E. A.; Wudl, F. Oligoacenes: theoretical prediction of open-shell singlet diradical ground states. *J. Am. Chem. Soc.* **2004**, *126*, 7416–7417.

(19) Van Setten, M. J.; Xenioti, D.; Alouani, M.; Evers, F.; Korytr, R. Incommensurate quantum size oscillations of oligoacene wires adsorbed on Au(111). *J. Phys. Chem. C* **2019**, *123*, 8902–8907.

(20) Eisenhut, F.; Khne, T.; Garca, F.; Fernndez, S.; Guitin, E.; Prez, D.; Trinquier, G.; Cuniberti, G.; Joachim, C.; Pea, D.; Moresco, F. Dodecacene generated on surface: reopening of the energy gap. *ACS Nano* **2020**, *14*, 1011–1017.

(21) Feng, Y.; Zhang, F.; Song, X.; Bu, Y. Molecular vibrations induced potential diradical character in hexazapentacene. *J. Phys. Chem. C* **2016**, *120*, 10215–10226.

(22) Posenitskiy, E.; Rapacioli, M.; Lepetit, B.; Lemoine, D.; Spiegelman, F. Non-adiabatic molecular dynamics investigation of the size dependence of the electronic relaxation in polyacenes. *Phys. Chem. Chem. Phys.* **2019**, *21*, 12139–12149.

(23) Song, M.; Song, X.; Bu, Y. Tuning the spin coupling interactions in the nitroxide-based bisphenol–like diradicals. *Chem. Phys. Chem.* **2017**, *18*, 2487–2498.

(24) Ali, M. E.; Datta, S. N. Broken-symmetry density functional theory investigation on bis-nitronyl nitroxide diradicals: influence of length and aromaticity of couplers. *J. Phys. Chem. A* **2006**, *110*, 2776–2784.

(25) Kolanji, K.; Ravat, P.; Bogomyakov, A. S.; Ovcharenko, V. I.; Schollmeyer, D.; Baumgarten, M. Mixed phenyl and thiophene oligomers for bridging nitronyl nitroxides. *J. Org. Chem.* **2017**, *82*, 7764–7773.

(26) Feng, Y.; Zhang, F.; Song, X.; Bu, Y. Diradicalized biphenyl derivative carbon-based material molecules: exploring the tuning effects on magnetic couplings. *Phys. Chem. Chem. Phys.* **2017**, *19*, 5932–5943.

(27) Lee, C.; Yang, W.; Parr, R. G. Development of the Colle-Salvetti correlation-energy formula into a functional of the electron density. *Phys. Rev. B* **1988**, *37*, 785–789.

(28) Hellweg, A.; Hättig, C.; Höfener, S.; Klopper, W. Optimized accurate auxiliary basis sets for RI-MP2 and RI-CC2 calculations for the atoms Rb to Rn. *Theor. Chem. Acc.* **2007**, *117*, 587–597.

(29) Weigend, F.; Ahlrichs, R. Balanced basis sets of split valence, triple zeta valence and quadruple zeta valence quality for H to Rn: Design and assessment of accuracy. *Phys. Chem. Chem. Phys.* **2005**, *7*, 3297–3305.

(30) Neese, F. Software update: the ORCA program system, version 4.0. *WIREs Comput. Mol. Sci.* **2018**, *8*, e1327.

(31) Neese, F.; Wennmohs, F.; Hansen, A.; Becker, U. Efficient, approximate and parallel Hartree–Fock and hybrid DFT calculations. A 'chain-of-spheres' algorithm for the Hartree-Fock exchange. *Chem. Phys.* **2009**, *356*, 98 – 109.

(32) Mitani, M.; Yamaki, D.; Takano, Y.; Kitagawa, Y.; Yoshioka, Y.; Yamaguchi, K. Density-functional study of intramolecular ferromagnetic interaction through m-phenylene coupling unit (II): Examination of functional dependence. *J. Chem. Phys.* **2000**, *113*, 10486–10504.

(33) Caballol, R.; Castell, O.; Illas, F.; de P. R. Moreira, I.; Malrieu, J. P. Remarks on the proper use of the broken symmetry approach to magnetic coupling. *J. Phys. Chem. A* **1997**, *101*, 7860–7866.

(34) Neese, F. Definition of corresponding orbitals and the diradical character in broken symmetry DFT calculations on spin coupled systems. *J. Phys. Chem. Solids* **2004**, *65*, 781 – 785.

(35) Noodleman, L. Valence bond description of antiferromagnetic coupling in transition metal dimers. *J. Chem. Phys.* **1981**, *74*, 5737–5743.

(36) Ko, K. C.; Cho, D.; Lee, J. Y. Scaling approach for intramolecular magnetic coupling constants of organic diradicals. *J. Phys. Chem. A* **2013**, *117*, 3561–3568.

(37) Valero, R.; Costa, R.; de P. R. Moreira, I.; Truhlar, D. G.; Illas, F. Performance of the M06 family of exchange-correlation functionals for predicting magnetic coupling in organic and inorganic molecules. *J. Chem. Phys.* **2008**, *128*, 114103.

(38) Noodleman, L.; Davidson, E. R. Ligand spin polarization and antiferromagnetic coupling in transition metal dimers. *Chem. Phys.* **1986**, *109*, 131 – 143.

(39) Ginsberg, A. P. Magnetic exchange in transition metal complexes. 12. Calculation of cluster exchange coupling constants with the X.alpha.-scattered wave method. *J. Am. Chem. Soc.* **1980**, *102*, 111–117.

(40) Noodleman, L.; Case, D. A.; Aizman, A. Broken symmetry analysis of spin coupling in iron-sulfur clusters. *J. Am. Chem. Soc.* **1988**, *110*, 1001–1005.

(41) Soda, T.; Kitagawa, Y.; Onishi, T.; Takano, Y.; Shigeta, Y.; Nagao, H.; Yoshioka, Y.; Yamaguchi, K. Ab initio computations of effective exchange integrals for H-H, H-He-H and Mn2O2 complex: comparison of broken-symmetry approaches. *Chem. Phys. Lett.* **2000**, *319*, 223 – 230.

(42) Yamanaka, S.; Okumura, M.; Nakano, M.; Yamaguchi, K. EHF theory of chemical reactions Part 4. UNO CASSCF, UNO CASPT2 and R(U)HF coupled-cluster (CC) wavefunctions. *J. Mol. Struct.* **1994**, *310*, 205–218.

(43) Reta, D.; Moreira, I. d. P. R.; Illas, F. Magnetic coupling constants in three electrons three centers problems from effective hamiltonian theory and validation of broken symmetry-based approaches. *J. Chem. Theory Comput.* **2016**, *12*, 3228–3235.

(44) Kaduk, B.; Kowalczyk, T.; Van Voorhis, T. Constrained density functional theory. *Chem. Rev.* **2012**, *112*, 321–370.

(45) Rudra, I.; Wu, Q.; Voorhis, T. V. Accurate magnetic exchange couplings in transition-metal complexes from constrained density-functional theory. *J. Chem. Phys.* **2006**, *124*, 024103.

(46) Valiev, M.; Bylaska, E.; Govind, N.; Kowalski, K.; Straatsma, T.; Dam, H. V.; Wang, D.; Nieplocha, J.; Apra, E.; Windus, T.; de Jong, W. NWChem: A comprehensive and scalable open-source solution for large scale molecular simulations. *Comput. Phys. Commun.* **2010**, *181*, 1477 – 1489.

(47) Ali, M. E.; Nair, N. N.; Staemmler, V.; Marx, D. Constrained spin-density dynamics of an iron-sulfur complex: ferredoxin cofactor. *J. Chem. Phys.* **2012**, *136*, 224101.

(48) Ali, M. E.; Staemmler, V.; Marx, D. Magnetostructural dynamics of rieske versus ferredoxin iron-sulfur cofactors. *Phys. Chem. Chem. Phys.* **2015**, *17*, 6289–6296.

(49) Dudarev, S. L.; Botton, G. A.; Savrasov, S. Y.; Humphreys, C. J.; Sutton, A. P. Electron-energy-loss spectra and the structural stability of nickel oxide: An LSDA+U study. *Phys. Rev. B* **1998**, *57*, 1505–1509.

(50) Anisimov, V. I.; Zaanen, J.; Andersen, O. K. Band theory and Mott insulators: Hubbard *U* instead of Stoner *I*. *Phys. Rev. B* **1991**, *44*, 943–954.

(51) Liechtenstein, A. I.; Anisimov, V. I.; Zaanen, J. Density-functional theory and strong interactions: Orbital ordering in Mott-Hubbard insulators. *Phys. Rev. B* **1995**, *52*, R5467–R5470.

(52) Anisimov, V. I.; Solovyev, I. V.; Korotin, M. A.; Czyżyk, M. T.; Sawatzky, G. A. Density-functional theory and NiO photoemission spectra. *Phys. Rev. B* **1993**, *48*, 16929–16934.

(53) Kresse, G.; Joubert, D. From ultrasoft pseudopotentials to the projector augmented-wave method. *Phys. Rev. B* **1999**, *59*, 1758–1775.

(54) Zhang, Y.; Jiang, H. Intra- and interatomic spin interactions by the density functional theory plus *U* approach: a critical assessment. *J. Chem. Theory Comput.* **2011**, *7*, 2795–2803.

(55) Rivero, P.; Loschen, C.; Moreira, I. D. P. R.; Illas, F. Performance of plane-wave-based LDA+*U* and GGA+*U* approaches to describe magnetic coupling in molecular systems. *J. Comput. Chem.* **2009**, *30*, 2316–2326.

(56) Kresse, G.; Furthmüller, J. Efficient iterative schemes for *ab initio* total-energy calculations using a plane-wave basis set. *Phys. Rev. B* **1996**, *54*, 11169–11186.

(57) Roos, B. O. The complete active space SCF method in a fock-matrix-based super-CI formulation. *Int. J. Quantum Chem.* **1980**, *18*, 175–189.

(58) Szalay, P. G.; Mller, T.; Gidofalvi, G.; Lischka, H.; Shepard, R. Multiconfiguration self-consistent field and multireference configuration interaction methods and applications. *Chem. Rev.* **2012**, *112*, 108–181.

(59) Suaud, N.; Ruamps, R.; Guihry, N.; Malrieu, J. P. A strategy to determine appropriate active orbitals and accurate magnetic couplings in organic magnetic systems. *J. Chem. Theory Comput.* **2012**, *8*, 4127–4137.

(60) Angeli, C.; Bories, B.; Cavallini, A.; Cimiraglia, R. Third-order multireference perturbation theory: The n-electron valence state perturbation-theory approach. *J. Chem. Phys.* **2006**, *124*, 054108.

(61) Evgeny, T.; Ashok, K.; Martin, B.; Sergey, V.; Matvey, F.; Dmitry, G.; Inna, S.; Nina, G. The design of radical stacks: nitronyl-nitroxide-substituted heteropentacenes. *Chemistry-Open* **2017**, *6*, 642–652.

(62) Ali, M. E.; Staemmler, V.; Illas, F.; Oppeneer, P. M. Designing the redox-driven switching of ferro- to antiferromagnetic couplings in organic diradicals. *J. Chem. Theory Comput.* **2013**, *9*, 5216–5220.

(63) Cho, D.; Ko, K. C.; Lee, J. Y. Quantum chemical approaches for controlling and evaluating intramolecular magnetic interactions in organic diradicals. *Int. J. Quantum Chem.* **2016**, *116*, 578–597.

(64) David, G.; Guihry, N.; Ferr, N. What are the physical contents of hubbard and heisenberg

hamiltonian interactions extracted from broken symmetry DFT calculations in magnetic compounds? *J. Chem. Theory Comput.* **2017**, *13*, 6253–6265.

(65) Bajaj, A.; Ali, M. E. First-principle design of blatters diradicals with strong ferromagnetic exchange interactions. *J. Phys. Chem. C* **2019**, *123*, 15186–15194.

(66) Ali, M. E.; Datta, S. N. Polyacene spacers in intramolecular magnetic coupling. *J. Phys. Chem. A* **2006**, *110*, 13232–13237.

(67) Bhattacharya, D.; Shil, S.; Misra, A.; Klein, D. J. Intramolecular ferromagnetic coupling in bis-oxoverdazyl and bis-thioxoverdazyl diradicals with polyacene spacers. *Theor. Chem. Acc.* **2010**, *127*, 1432–2234.

(68) Sarbadhikary, P.; Shil, S.; Misra, A. Magnetic and transport properties of conjugated and cumulated molecules: the π -system enlightens part of the story. *Phys. Chem. Chem. Phys.* **2018**, *20*, 9364–9375.

(69) Kaplan, I. G. Problems in DFT with the total spin and degenerate states. *Int. J. Quantum Chem.* **2007**, *107*, 2595–2603.

(70) Cano, J.; Lloret, F.; Julve, M. Theoretical design of magnetic wires from acene and nanocorone derivatives. *Dalton Trans.* **2016**, *45*, 16700–16708.

(71) Yamaguchi, K.; Okumura, M.; Takada, K.; Yamanaka, S. Instability in chemical bonds. II. Theoretical studies of exchange-coupled open-shell systems. *Int. J. Quantum Chem.* **1993**, *48*, 501–515.

(72) Khurana, R.; Bajaj, A.; Ali, M. E. How Plausible is getting Ferromagnetic Interactions by Coupling Blatter's Radical via its Fused Benzene Ring? *J. Phys. Chem. A* **2020**, acs.jpca.0c05719.

(73) Jiang, D.; Dai, S. Electronic ground state of higher acenes. *J. Phys. Chem. A* **2008**, *112*, 332–335.

(74) Sharma, P.; Bernales, V.; Knecht, S.; Truhlar, D. G.; Gagliardi, L. Density matrix renormalization group pair-density functional theory (DMRG-PDFT): singlet-triplet gaps in polyacenes and polyacetylenes. *Chem. Sci.* **2019**, *10*, 1716–1723.

(75) Nagami, T.; Fujiyoshi, J.; Tonami, T.; Watanabe, K.; Yamane, M.; Okada, K.; Kishi, R.; Nakano, M.; Champagne, B.; Ligeois, V. Evaluation of aromaticity for open-shell singlet dicyclopenta-fused acenes and polyacenes based on a magnetically induced current. *Chem. Eur. J.* **2018**, *24*, 13457–13466.

(76) Trinquier, G.; David, G.; Malrieu, J. P. Qualitative views on the polyradical character of long acenes. *J. Phys. Chem. A* **2018**, *122*, 6926–6933.